Supplementary Information

Acoustically Shaped DNA-Programmable Materials

Z.A. Arnon[1], S. Piperno[2], D.C. Redeker[1], E. Randall[1], A.V. Tkachenko[3], H. Shpaisman[2] and O. Gang[1,3,4*]
[1]Department of Chemical Engineering, Columbia University, New York, NY, USA
[2]Department of Chemistry and Institute for Nanotechnology and Advanced Materials, Bar-Ilan University, Ramat Gan, Israel
[3]Center for Functional Nanomaterials, Brookhaven National Laboratory, Upton, NY, USA
[4]Department of Applied Physics and Applied Mathematics, Columbia University, New York, NY, USA
*og2226@columbia.edu

Supplementary Methods

Acoustic Transducer

A Y+128° X-propagation lithium niobate (LiNbO3) wafer (500 μm thick) was coated with a layer of AZ5214 photoresist (MicroChem, Newton, MA) through spin-coating. The coated wafer underwent lithography using a maskless aligner (MLA 150-Heidelberg) for precise patterning and later treated with a photoresist developer (Microchem AZ726) for development. Subsequently, an e-beam evaporator (Bestec) was used to deposit a double metal layer (Cr/Au, 100Å/1000Å) onto the wafer. Following this procedure, a lift-off process was employed to create the interdigital transducers (IDTs).

Crystallites Orientations

Images of before and after the acoustic field was applied were used to assess the orientation of crystals, as seen in Supplementary Figure 2. The angle measured was from the parallel to the capillary wall. The chosen angle was always between 0°-45° as shown in Figure 2a. Analysis was performed using *Fiji*[1] *(version 1.54f)*.

Small-Angle X-ray Scattering (SAXS) of Assembled Structures

The SAXS measurements were performed at the Complex Materials Scattering (CMS) beamline at the National Synchrotron Light Source II (NSLS-II) at Brookhaven National Laboratory (BNL) in Upton, NY. The 2D scattering data was collected on area detectors located downstream of the sample's position. Area images were integrated into a one-dimensional (1D) $I(q)$ scattering curve as a function of the scattering vector q, where $q = 4\frac{\pi}{\lambda}\sin\left(\frac{\theta}{2}\right)$ with λ and θ being the wavelength of the incident X-rays and the full scattering angle, respectively. The resultant 1D curves spanned

roughly 0.04 nm^{-1} to 1 nm^{-1} with a resolution of 0.002 nm^{-1}. The structure factor $S(q)$ was obtained by dividing $I(q)$ by the corresponding particle form factor $P(q)$.

Beamline	11-BM CMS
Photon Energy (keV)	13.5
Horizontal × Vertical Beam size (μm × μm)	200 x 200
Approximate Flux (photons/sec)	10^{11}
Sample-to-Detector Distance (m)	5.05
Detector Manufacturer	Dectris
Detector Model	Pilatus 1M
Detector Pixel Size (μm x μm)	172 x 172

Supplementary Table 1. X-ray beam characteristics and setup details at the CMS (NSLS-II) beamline

In this work, we implement modeling of the presented analysis using the ScatterSim software package, a python package that implements a scattering formalism for superlattices[2,3]. This formalism can generically model the scattering from arbitrary anisotropic nano-objects within the unit cell of a regular superlattice. We used this library to perform the modeling for the simple cubic crystal, with the code being available for download on Git Hub[3].

Supplementary Discussion

Acoustic Field Considerations

SAWs are generated by IDTs fabricated with photolithography to convert electrical signals into acoustic waves through the piezoelectric effect of a substrate. The acoustic force applied on particles is dependent on the acoustic contrast between the medium and particles, which is sufficient for most systems of particles in aqueous media. The SSAW-induced pressure generates a force F_{ac}, applied on small particles, has a form:

$$F_{ac} = \frac{4}{3}\pi r^3 E_{ac} q \sin(2kx)\phi$$

where r is the radius of the particle, E_{ac} is the acoustic energy density, q is the wave number, x is the distance of the particle from the node and ϕ is the acoustic contrast factor between the particle and the medium (water).

Acoustic contrast factor

To estimate the acoustic contrast factor ϕ of our material, we first consider a hypothetical case when DNA origami fills entire volume of the frame. The density ratio of DNA to water is approximately $\rho_{DNA}/\rho_{H_2O} \approx 1.7$ which corresponds to

$$\phi_{DNA} = \frac{5\rho_{DNA} - 2\rho_{H_2O}}{2\rho_{DNA} + \rho_{H_2O}} - \frac{\beta_{DNA}}{\beta_{H_2O}} \approx 1.5 - \frac{\beta_{DNA}}{\beta_{H_2O}}$$

where β_{DNA}/β_{H_2O} is the compressibility ratio of DNA to water. Since we know, based on experimental evidence, that gold particles and DNA frames are pushed to the same locations (Supplementary Figure 4), we can conclude that ϕ_{DNA} is positive. Hence, the compressibility ratio $\frac{\beta_{DNA}}{\beta_{H_2O}}$ is between 0 and 1.5. Plotting a particle edge length threshold (L*) vs the compressibility ratio (Supplementary Figure 5) shows that even for energy of 200 J/m^3 (See 'Acoustic Force Considerations'), individual particles need to be well above a threshold of 30 nm in order for the acoustic force to push them efficiently.

Acoustic Force Considerations

The force applied by the waves on particles is dependent on the position of the particle, where at specific $n\pi$ locations called the 'nodes', the force will be reduced to zero. Small particles with positive acoustic contrast around the nodes are pushed into the nodes, where they will stay for as long as the wave is applied. As estimated above, the contrast factors for individual DNA frames as well as for the larger self-assembled structures are expected be close to the volume fraction of DNA in them, *i.e.* $\phi \sim 0.1$. For a particle to be affected by the SSAW, its energy difference between the node and antinode positions, $VE_{ac}\phi$, must exceed kT. To estimate the particles size threshold (L*) that will be affected by the acoustic force, the acoustic energy density (E_{ac}) must be estimated first. By using polystyrene beads of 1 μm (Supplementary Movie 5) and calculating the velocity of the beads under the acoustic force, we estimated that the acoustic energy density is $E_{ac} \simeq 50 J/m^3$ (for more details on the calculation, see Supplementary Table 2). This corresponds to the particle size range of $L \gtrsim \left(\frac{kT}{E_{ac}\phi}\right)^{\frac{1}{3}} \simeq 80\ nm$ (Supplementary Figure 5). This means that individual DNA frames (~30 nm) should not be affected, while the crystalline particles larger than the critical nucleus typically are.

Parameter	Description	Equation	Value
$\rho\ (kg/m^3)$	Density of polystyrene particles	-	1050
ϕ_w	Acoustic contrast of polystyrene in water	-	0.193
$r\ (m)$	Radius of polystyrene particles	-	0.5e-6
$\eta\ (N \cdot s/m^2)$	Viscosity	-	6.5e-4
$d\ (m)$	Distance particles travel (from movie S5)	-	75e-6
$t\ (s)$	Time for particles to travel (from movie S5)	-	18
$v\ (m/s)$	Velocity	d/t	4.16e-6
$F_{drag}\ (N)$	Drag force	$6\pi\eta rv$	2.55e-14
$m\ (kg)$	Particle mass	$\frac{4}{3}\pi r^3\rho$	5.5e-16
$F_{calculated}\ (N)$	Total force on particles	$m \cdot a$	1.27e-22
$F_{ac}\ (N)$	Acoustic force on particles	$F_{calculated}+F_{drag}$	2.55e-14
$q\ (m^{-1})$	Wavenumber	$1/\lambda$	5000
$E_{ac}\ (J/m^3)$	Acoustic Energy Density	$\frac{3}{4\pi r^3 qsin(2kx)\phi_w} \cdot F_{ac}$	50.5

Supplementary Table 2. Acoustic energy density calculation table. The acoustic force calculation was performed for microparticles with a known diameter, density, compressibility and acoustic contrast factor[4] in a capillary tube filled with water (0.05 x 1 mm). IDT 19.34 MHz and Amplitude of 20Vpp. The velocity and acceleration of the particles were calculated by measuring the time it takes for the particles to cover a known distance. We used the time it takes all dispersed particles to reach the nodes and considered half the node distance as travel distance.

Theoretical Modelling Parameters

The table below (Supplementary Table 3) lists the parameters used for modeling. Out of them, Γ was used as a tuning parameter for the unmodified nucleation and growth theory that describes the no-wave data. Two additional fitting parameters are specific to the infusion model. The rest of the parameters were determined based on the known geometrical and thermodynamic properties of the building blocks, and the experimental conditions. In particular, the diffusion coefficient was determined by Einstein relationship (by setting hydrodynamic radius to a):

$D = \frac{kT}{6\pi\eta a} = 5.9 \cdot 10^{-12}\frac{m^2}{s}$. The sequence-specific hybridization entropy of each DNA duplex was found to be $160\frac{cal}{K \cdot mol}$. There are 4 DNA duplexes in each bond, and 3 bonds per octahedral building block in the cubic lattice, which gives:

$$\Delta S/kT = \frac{12 \cdot 160\frac{cal}{K \cdot mol}}{RT} = 3.0\ K^{-1}.$$

Parameter	a	c_0	D	$\Delta S/kT$	Γ	ε	κ
Value	$40\ nm$	40 nM	$5.9 \cdot 10^{-12}\frac{m^2}{s}$	$3.0\ K^{-1}$	7.5 (fitting)	400 (fitting)	$0.0005\ s^{-1}$ (fitting)

Supplementary Table 3. Parameters for the theoretical model used in the study.

Supplementary Tables

Internal DNA Staples

Sequence Name	Sequence
OCT-Staple-1	GCCTTGAATCTTTTCCGGAACCGCCTCCCAGAGCCCAGAGCCGCCGCCAGCATT
OCT-Staple-2	ATAAGGCGCCAAAAGTTGAGATTTAGGATAACGGACCAGTCA
OCT-Staple-3	GATGGTTGGGAAGAAAAATCCACCAGAAATAATTGGGCTTGA
OCT-Staple-4	GGACGTTTAATTTCGACGAGAAACACCACCACTAATGCAGAT
OCT-Staple-5	ATTTTAAGAACTGGCTTGAATTATCAGTGA
OCT-Staple-6	TCAGAACCGCCACCCTCTCAGAGTATTAGC
OCT-Staple-7	TCAGAGCGCCACCACATAATCAAAATCAGAACGAGTAGTATG
OCT-Staple-8	AACCAGACGCTACGTTAATAAAACGAACATACCACATTCAGG
OCT-Staple-9	GTTTGCCTATTCACAGGCAGGTCAGACGCCACCACACCACCC
OCT-Staple-10	ACATAACTTGCCCTAACTTTAATCATTGCATTATAACAACATTATTACAGGTAG
OCT-Staple-11	CATGTCACAAACGGCATTAAATGTGAGCAATTCGCGTTAAAT
OCT-Staple-12	AAGATTGTTTTTTAACCAAGAAACCATCGACCCAAAAACAGG
OCT-Staple-13	CAGCTCATATAAGCGTACCCCGGTTGATGTGTCGGATTCTCC
OCT-Staple-14	GTTAAAATTCGCATTATAAACGTAAACTAG
OCT-Staple-15	AGCACCATTACCATTACAGCAAATGACGGA
OCT-Staple-16	GTCACCAGAGCCATGGTGAATTATCACCAATCAGAAAAGCCT
OCT-Staple-17	CCGACTTATTAGGAACGCCATCAAAAATGAGTAACAACCCCA
OCT-Staple-18	AATTATTGTTTTCATGCCTTTAGCGTCAGATAGCACGGAAAC
OCT-Staple-19	CTTCGCTGGGCGCAGACGACAGTATCGGGGCACCGTCGCCATTCAGGCTGCGCA
OCT-Staple-20	ACAAAGAAATTTAGGTAGGGCTTAATTGTATACAACGGAATC
OCT-Staple-21	TGACCTACTAGAAAAAGCCCCAGGCAAAGCAATTTCATCTTC
OCT-Staple-22	ATAATTAAATTTAAAAAACTTTTTCAAACTTTTAACAACGCC
OCT-Staple-23	AGGCGTTAAATAAGAAGACCGTGTCGCAAG
OCT-Staple-24	TGCCGGAAGGGGACTCGTAACCGTGCATTATATTTTAGTTCT
OCT-Staple-25	CTCCAGCCAGCTTTCCCCTCAGGACGTTGG
OCT-Staple-26	CAGTTTGAATGTTTAGTATCATATGCGTAGAATCGCCATAGC
OCT-Staple-27	TGTAGATATTACGCGGCGATCGGTGCGGGCGCCATCTTCTGG
OCT-Staple-28	AACATGTACGCGAGTGGTTTGAAATACCTAAACACATTCTTACCAGTATAAAGC
OCT-Staple-29	CGCTGGTGCTTTCCTGAATCGGCCAACGAGGGTGGTGATTGCCCTTCACCGCCT
OCT-Staple-30	AACAAAAATAACTAGGTCTGAGAGACTACGCTGAGTTTCCCT
OCT-Staple-31	AACAGTACTTGAAAACATATGAGACGGGTCTTTTTTAATGGA
OCT-Staple-32	TAGAATCCATAAATCATTTAACAATTTCTCCCGGCTTAGGTT
OCT-Staple-33	GTAAATCGTCGCTATTGAATAACTCAAGAA
OCT-Staple-34	TTGCGTATTGGGCGCCCGCGGGGTGCGCTC
OCT-Staple-35	TTTCACCGCATTAAAGTCGGGAAACCTGATTTGAATTACCCA
OCT-Staple-36	GCCAGCTAGGCGATAGCTTAGATTAAGACCTTTTTAACCTGT
OCT-Staple-37	ACTGCCCTTGCCCCGTTGCAGCAAGCGGCAACAGCTTTTTCT
OCT-Staple-38	GGGTTATTTAATTACAATATATGTGAGTAATTAATAAGAGTCAATAGTGAATTT
OCT-Staple-39	TCCAAATCTTCTGAATTATTTGCACGTAGGTTTAACGCTAACGAGCGTCTTTCC

OCT-Staple-40	CAGATATTACCTGAATACCAAGTTACAATCGGGAGCTATTTT
OCT-Staple-41	ACGCGAGGCTACAACAGTACCTTTTACAAATCGCGCAGAGAA
OCT-Staple-42	GCACCCAGCGTTTTTTATCCGGTATTCTAGGCGAATTATTCA
OCT-Staple-43	AAGCCTTAAATCAAGACTTGCGGAGCAAAT
OCT-Staple-44	ATTGCGTAGATTTTCAAAACAGATTGTTTG
OCT-Staple-45	TGAATATTATCAAAATAATGGAAGGGTTAATATTTATCCCAA
OCT-Staple-46	CCTACCAACAGTAATTTTATCCTGAATCAAACAGCCATATGA
OCT-Staple-47	GATTATAAAGAAACGCCAGTTACAAAATTTACCAACGTCAGA
OCT-Staple-48	TTTCAATAGAAGGCAGCGAACCTCCCGATTAGTTGAAACAATAACGGATTCGCC
OCT-Staple-49	GATATTCTAAATTGAGCCGGAACGAGGCCCAACTTGGCGCATAGGCTGGCTGAC
OCT-Staple-50	GGTTGATTTTCCAGCAGACAGCCCTCATTCGTCACGGGATAG
OCT-Staple-51	AGTACCGAATAGGAACCCAAACGGTGTAACCTCAGGAGGTTT
OCT-Staple-52	CAAGCCCCCACCCTTAGCCCGGAATAGGACGATCTAAAGTTT
OCT-Staple-53	CAGAGCCACCACCCTCTCAGAACTCGAGAG
OCT-Staple-54	AAGGGAACCGAACTGAGCAGACGGTATCAT
OCT-Staple-55	GGACAGAGTTACTTTGTCGAAATCCGCGTGTATCACCGTACG
OCT-Staple-56	GCTCCATTGTGTACCGTAACACTGAGTTAGTTAGCGTAACCT
OCT-Staple-57	CGCCTGAATTACCCTAATCTTGACAAGACAGACCATGAAAGA
OCT-Staple-58	TGTCGTCATAAGTACAGAACCGCCACCCATTTTCACAGTACAAACTACAACGCC
OCT-Staple-59	ATGACCACTCGTTTGGCTTTTGCAAAAGTTAGACTATATTCATTGAATCCCCCT
OCT-Staple-60	GTAATACGCAAACATGAGAGATCTACAACTAGCTGAGGCCGG
OCT-Staple-61	AGAACCCCAAATCACCATCTGCGGAATCGAATAAAAATTTTT
OCT-Staple-62	AGACAGTTCATATAGGAGAAGCCTTTATAACATTGCCTGAGA
OCT-Staple-63	GTAAAGATTCAAAAGGCCTGAGTTGACCCT
OCT-Staple-64	GGTAATAGTAAAATGTAAGTTTTACACTAT
OCT-Staple-65	GTCCAATAGCGAGAACCAGACGACGATATTCAACGCAAGGGA
OCT-Staple-66	CCAAAATACAATATGATATTCAACCGTTAGGCTATCAGGTAA
OCT-Staple-67	CATAACCTAAATCAACAGTTCAGAAAACGTCATAAGGATAGC
OCT-Staple-68	GTCTGGATTTTGCGTTTTAAATGCAATGGTGAGAAATAAATTAATGCCGGAGAG
OCT-Staple-69	GGGCGACCCCAAAAGTATGTTAGCAAACTAAAAGAGTCACAATCAATAGAAAAT
OCT-Staple-70	TATAAAGCATCGTAACCAAGTACCGCACCGGCTGTAATATCC
OCT-Staple-71	CAACATGATTTACGAGCATGGAATAAGTAAGACGACAATAAA
OCT-Staple-72	CATCCTATTCAGCTAAAAGGTAAAGTAAAAAGCAAGCCGTTT
OCT-Staple-73	GATAAGTCCTGAACAACTGTTTAAAGAGAA
OCT-Staple-74	TAAAGGTGGCAACATAGTAGAAAATAATAA
OCT-Staple-75	AGACACCTTACGCAGAACTGGCATGATTTTCTGTCCAGACAA
OCT-Staple-76	CTCCTTAACGTAGAAACCAATCAATAATTCATCGAGAACAGA
OCT-Staple-77	CGGAATAATTCAACCCAGCGCCAAAGACTTATTTTAACGCAA
OCT-Staple-78	TTATTTTTACCGACAATGCAGAACGCGCGAAAAATCTTTCCTTATCATTCCAAG
OCT-Staple-79	CAGCCTTGGTTTTGTATTAAGAGGCTGACTGCCTATATCAGA
OCT-Staple-80	GGAAGCGCCCACAAACAGTTAATGCCCCGACTCCTCAAGATA
OCT-Staple-81	GAGATAACATTAGAAGAATAACATAAAAAGGAAGGATTAGGA
OCT-Staple-82	GTCAGAGGGTAATTGAGAACACCAAAATAG

OCT-Staple-83	AAGTTTTAACGGGGTCGGAGTGTAGAATGG
OCT-Staple-84	CAGTGCCTACATGGGAATTTACCGTTCCACAAGTAAGCAGAT
OCT-Staple-85	AGCGTCACGTATAAGAATTGAGTTAAGCCCTTTTTAAGAAAG
OCT-Staple-86	AAAGCGCCAAAGTTTATCTTACCGAAGCCCAATAATGAGTAA
OCT-Staple-87	TGCTAAACAGATGAAGAAACCACCAGAATTTAAAAAAAGGCT
OCT-Staple-88	GAGAATAGAGCCTTACCGTCTATCAAATGGAGCGGAATTAGA
OCT-Staple-89	CCAAAAGGAAAGGACAACAGTTTCAGCGAATCATCATATTCC
OCT-Staple-90	TTCACGTTGAAAATCTTGCGAATGGGATTT
OCT-Staple-91	GTCCACTATTAAAGAACCAGTTTTGGTTCC
OCT-Staple-92	TCAAAGGGAGATAGCCCTTATAAATCAAGACAACAACCATCG
OCT-Staple-93	ATAGCCCGCGAAAATAATTGTATCGGTTCGCCGACAATGAGT
OCT-Staple-94	GAAATCGATAACCGGATACCGATAGTTGTATCAGCTCCAACG
OCT-Staple-95	ATTAAGTATAAAGCGGCAAGGCAAAGAAACTAATAGGGTACC
OCT-Staple-96	CACGACGAATTCGTGTGGCATCAATTCTTTAGCAAAATTACG
OCT-Staple-97	CAGGTCGACTCTAGAGCAAGCTTCAAGGCG
OCT-Staple-98	TAACCTGTTTAGCTATTTTCGCATTCATTC
OCT-Staple-99	GAGCTCGTTGTAAACGCCAGGGTTTTCCAAAGCAATAAAGCC
OCT-Staple-100	CGCGAGCTTAGTTTTTCCCAATTCTGCGCAAGTGTAAAGCCT
OCT-Staple-101	AGTAGATTGAAAAGAATCATGGTCATAGCCGGAAGCATAAGT
OCT-Staple-102	CATATAACTAATGAACACAACATACGAGCTGTTTCTTTGGGG
OCT-Staple-103	ATGTTTTGCTTTTGATCGGAACGAGGGTACTTTTTCTTTTGATAAGAGGTCATT
OCT-Staple-104	AGAAGCAACCAAGCCAAAAGAATACACTAATGCCAAAACTCC
OCT-Staple-105	GAGGAAGCAGGATTCGGGTAAAATACGTAAAACACCCCCCAG
OCT-Staple-106	AACAGGTCCCGAAATTGCATCAAAAAGATCTTTGATCATCAG
OCT-Staple-107	TCAAAGCGAACCAGACCGTTTTATATAGTC
OCT-Staple-108	GCTTTGAGGACTAAAGAGCAACGGGGAGTT
OCT-Staple-109	AAGTTTCAGACAGCCGGGATCGTCACCCTTCTGTAGCTCAAC
OCT-Staple-110	CAGCGAACATTAAAAGAGAGTACCTTTACTGAATATAATGAA
OCT-Staple-111	AAAGGCCAAATATGTTAGAGCTTAATTGATTGCTCCATGAGG
OCT-Staple-112	CGATTATAAGCGGAGACTTCAAATATCGCGGAAGCCTACGAAGGCACCAACCTA
OCT-Staple-113	GGGGTGCCAGTTGAGACCATTAGATACAATTTTCACTGTGTGAAATTGTTATCC
OCT-Staple-114	TCAGAGCTGGGTAAACGACGGCCAGTGCGATCCCCGTAGTAGCATTAACATCCA
OCT-Staple-115	TTAGCGGTACAGAGCGGGAGAATTAACTGCGCTAATTTCGGAACCTATTATTCT
OCT-Staple-116	TGATTATCAACTTTACAACTAAAGGAATCCAAAAAGTTTGAGTAACATTATCAT
OCT-Staple-117	GTAGCGCCATTAAATTGGGAATTAGAGCGCAAGGCGCACCGTAATCAGTAGCGA
OCT-Staple-118	AGCCGAAAGTCTCTCTTTTGATGATACAAGTGCCTTAAGAGCAAGAAACAATGA
OCT-Staple-119	GTGGGAAATCATATAAATATTTAAATTGAATTTTTGTCTGGCCTTCCTGTAGCC
OCT-Staple-120	CCCACGCGCAAAATGGTTGAGTGTTGTTCGTGGACTTGCTTTCGAGGTGAATTT

87 **Supplementary Table 4**. Sequence list of produced DNA origami octahedron structure. Without further strands
88 ('sticky ends'), this DNA structure will not be capable of binding to other origami.

External Staples ('Sticky Ends')

Sequence Name	Sequence
Vertex A-1	AGAGCCTAATTTGATTTTTTGTTTAAATCCTGAAATAAAGAATTTTTTTTTTTTTTTTTTTTT + (Binding Sequence)
Vertex A-2	TGTAGCATTCCAACGTTAGTAAATGAAGTGCCGCGCCACCCTTTTTTTTTTTTTTTTTTTTTT + (Binding Sequence)
Vertex A-3	GAAACATGAAAGCTCAGTACCAGGCGAAAAATGCTGAACAAATTTTTTTTTTTTTTTTTTTTT + (Binding Sequence)
Vertex A-4	TTTGCGGAACAATGGCAATTCATCAATCTGTATAATAATTTTTTTTTTTTTTTTTTTTTTT + (Binding Sequence)
Vertex B-1	AAAGATTCATCAGGAATTACGAGGCATGCTCATCCTTATGCGTTTTTTTTTTTTTTTTTTTT + (Binding Sequence)
Vertex B-2	CTTCATCAAGAGAAATCAACGTAACAGAGATTTGTCAATCATTTTTTTTTTTTTTTTTTTTT + (Binding Sequence)
Vertex B-3	CAAATGCTTTAAAAAATCAGGTCTTTAAGAGCAGCCAGAGGGTTTTTTTTTTTTTTTTTTTT + (Binding Sequence)
Vertex B-4	AAACGAAAGAGGGCGAAACAAAGTACTGACTATATTCGAGCTTTTTTTTTTTTTTTTTTTTT + (Binding Sequence)
Vertex C-1	AGCTTTCATCAACGGATTGACCGTAAAATCGTATAATATTTTTTTTTTTTTTTTTTTTTT + (Binding Sequence)
Vertex C-2	ACTGTTGGGAAGCAGCTGGCGAAAGGATAGGTCAAGATCGCATTTTTTTTTTTTTTTTTTTT + (Binding Sequence)
Vertex C-3	GGTAGCTATTTTAGAGAATCGATGAAAACATTAAATGTGTAGTTTTTTTTTTTTTTTTTTTT + (Binding Sequence)
Vertex C-4	ATAAATCATACATAAATCGGTTGTACTGTGCTGGCATGCCTGTTTTTTTTTTTTTTTTTTTT + (Binding Sequence)
Vertex D-1	TGATTGCTTTGAGCAAAAGAAGATGAAATAGCAGAGGTTTTGTTTTTTTTTTTTTTTTTTTT + (Binding Sequence)
Vertex D-2	AACGGGTATTAAGGAATCATTACCGCCAGTAATTCAACAATATTTTTTTTTTTTTTTTTTTTT + (Binding Sequence)
Vertex D-3	CAACGCTCAACAGCAGAGGCATTTTCAATCCAATGATAAATATTTTTTTTTTTTTTTTTTTTT + (Binding Sequence)
Vertex D-4	ATCAAAATCATATATGTAAATGCTGAACAAACACTTGCTTCTTTTTTTTTTTTTTTTTTTTT + (Binding Sequence)
Vertex E-1	GGCCCTGAGAGAAGCAGGCGAAAATCATTGCGTAGAGGCGGTTTTTTTTTTTTTTTTTTTTT + (Binding Sequence)
Vertex E-2	CTTAAACAGCTTATATATTCGGTCGCTTGATGGGGAACAAGATTTTTTTTTTTTTTTTTTTTT + (Binding Sequence)
Vertex E-3	GCTCACAATTCCGTGAGCTAACTCACTGGAAGTAATGGTCAATTTTTTTTTTTTTTTTTTTTT + (Binding Sequence)
Vertex E-4	TTTGCGGATGGCCAACTAAAGTACGGGCTTGCAGCTACAGAGTTTTTTTTTTTTTTTTTTTT + (Binding Sequence)
Vertex F-1	GACAGGAGGTTGAAACAAATAAATCCGCCCCCTCCGCCACCCTTTTTTTTTTTTTTTTTTTT + (Binding Sequence)
Vertex F-2	CAGAATCAAGTTTCGGCATTTTCGGTTAAATATATCACCAGTTTTTTTTTTTTTTTTTTTTT +

	(Binding Sequence)
Vertex F-3	TCATATGGTTTACGATTGAGGGAGGGAAACGCAATACATACATTTTTTTTTTTTTTTTTTTTT + (Binding Sequence)
Vertex F-4	AATAGCAATAGCACCAGAAGGAAACCTAAAGCCACTGGTAATTTTTTTTTTTTTTTTTTTTT + (Binding Sequence)
Binding Sequence A	ACCTACAC
Binding Sequence B	GTGTAGGT

Supplementary Table 5. Externally facing sticky ends located at the 6 vertices of the octahedron origami frame. There are 4 sequences (1-4) present at each vertex (A-F), where our designs keep the 'Binding Sequence' the same for these 4 sequences. The Binding Sequences are listed at the end of the tables.

Supplementary Figures

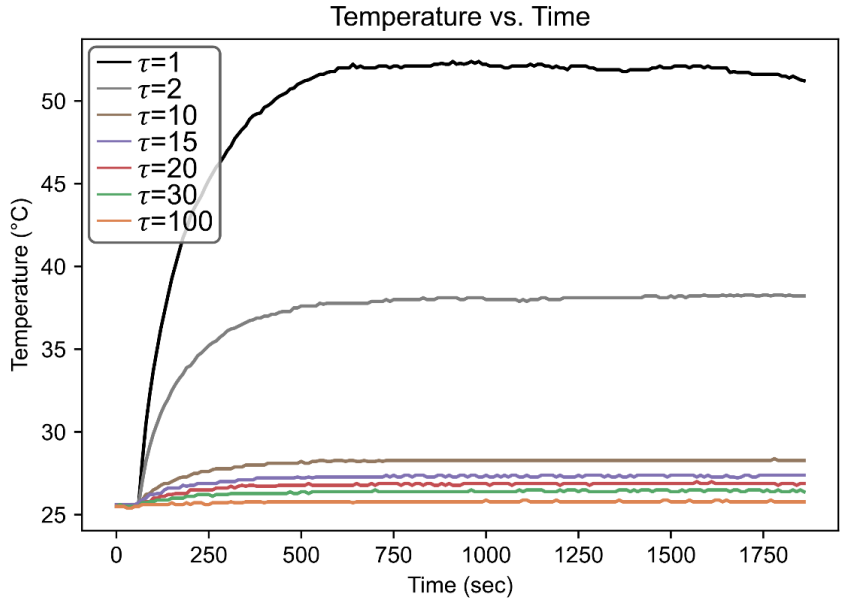

Supplementary Figure 1. Temperature change induced by the acoustic waves in the active region. τ is defined as the period divided by the pulse length. τ=1 means constant waves are applied. Waves were applied after 60 seconds at room temperature (25.5 °C) without the use of active temperature control. τ values in the experiments conducted were between 10 – 100. Thermal paste was used to ensure proper temperature measurement of the active region.

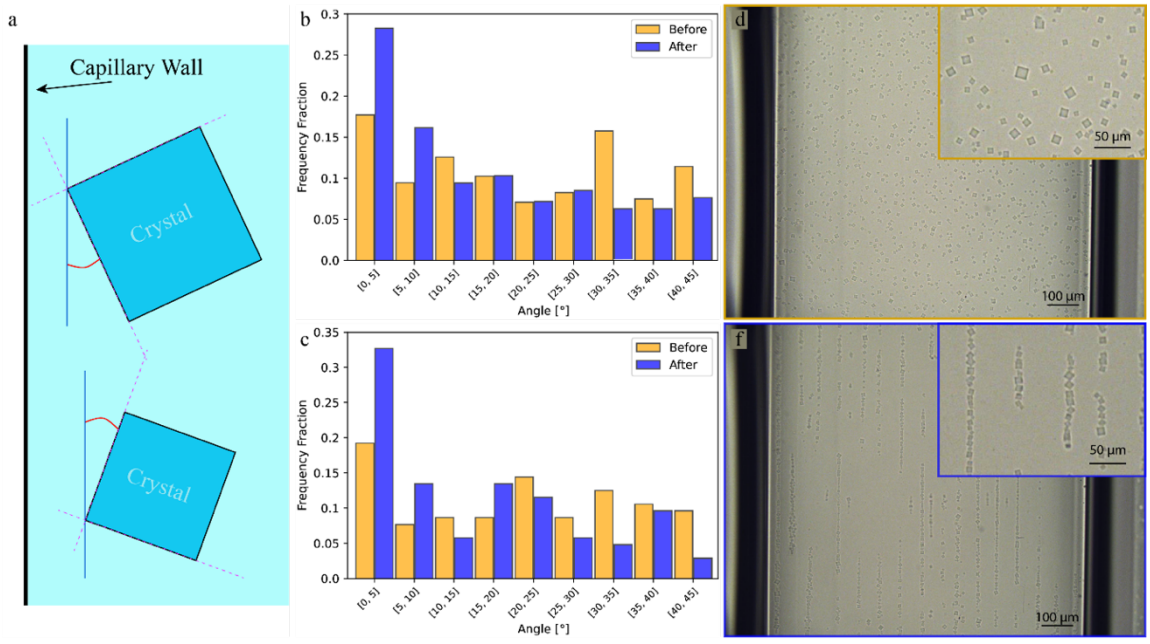

Supplementary Figure 2. Orientation of crystals before and after acoustic organization. **a.** Schematic of how the orientation of crystals was measured. The angle is always between 0° to 45°. **b,c.** Histogram of two separate experiments where the angles of individual crystals were measured before and after acoustic waves were applied. Panel b Before n=254, After n=223; Panel c Before n=104, After n=104. **d,f.** Images corresponding to the Histogram in panel b, before (d) and after (f) the acoustic waves. The Histogram in panel (c) corresponded to Supplementary Movie 2.

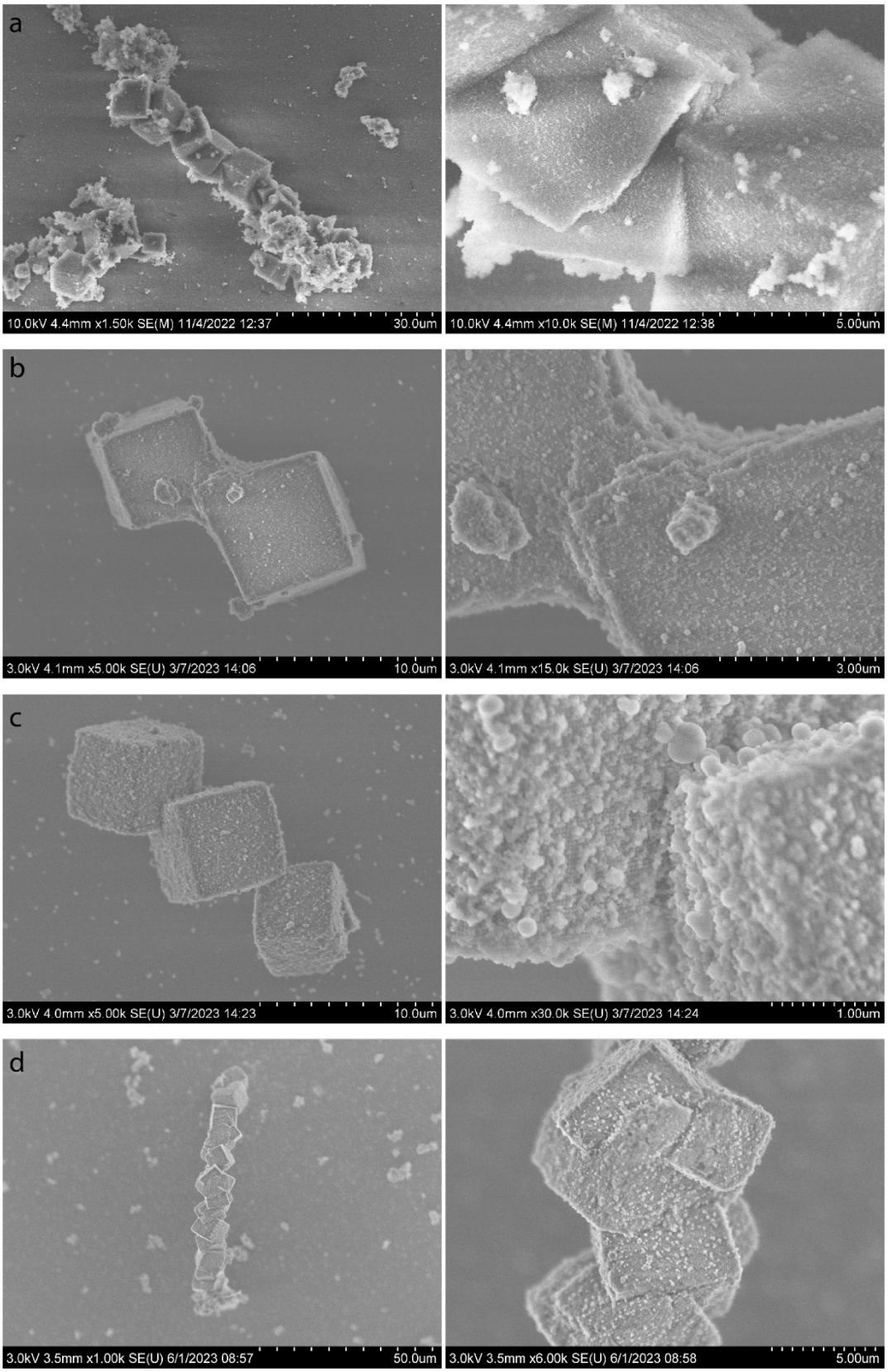

Supplementary Figure 3. **a-d.** Additional SEM images of fused crystals after reannealing. Zoomed-out (left) and zoomed-in (right) images of the same region.

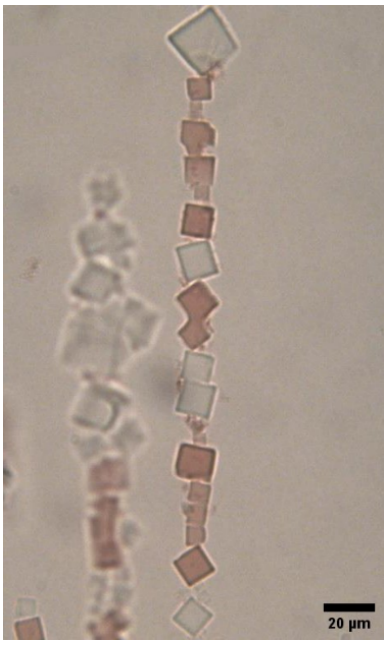

Supplementary Figure 4. Crystals are arranged linearly by acoustic field. Crystals filled with AuNPs are red, while empty crystals are clear.

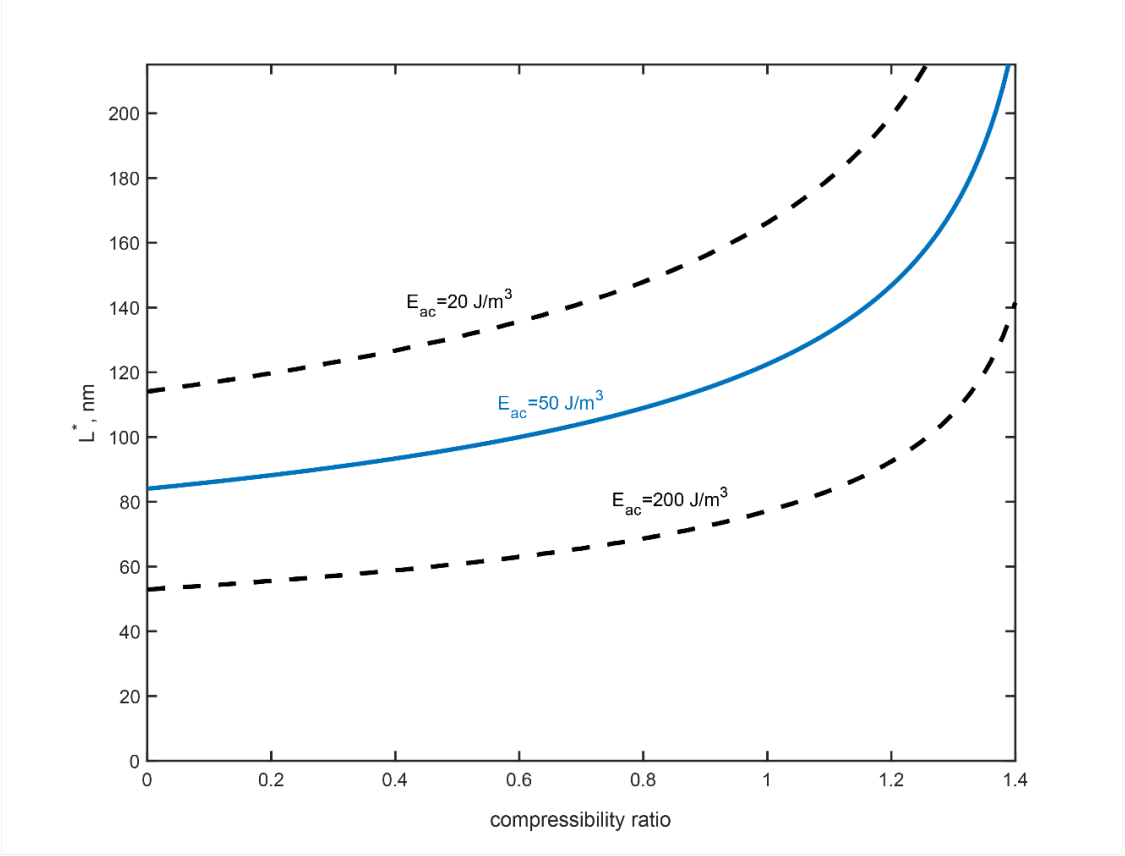

Supplementary Figure 5. Edge length threshold (L*) vs the compressibility ratio (β_{DNA}/β_{H_2O}) calculated for a range of acoustic energy densities between 20 and 200 J/m^3, where 50 J/m^3 (blue) is the estimated energy density for this study (Supplementary Table 2).

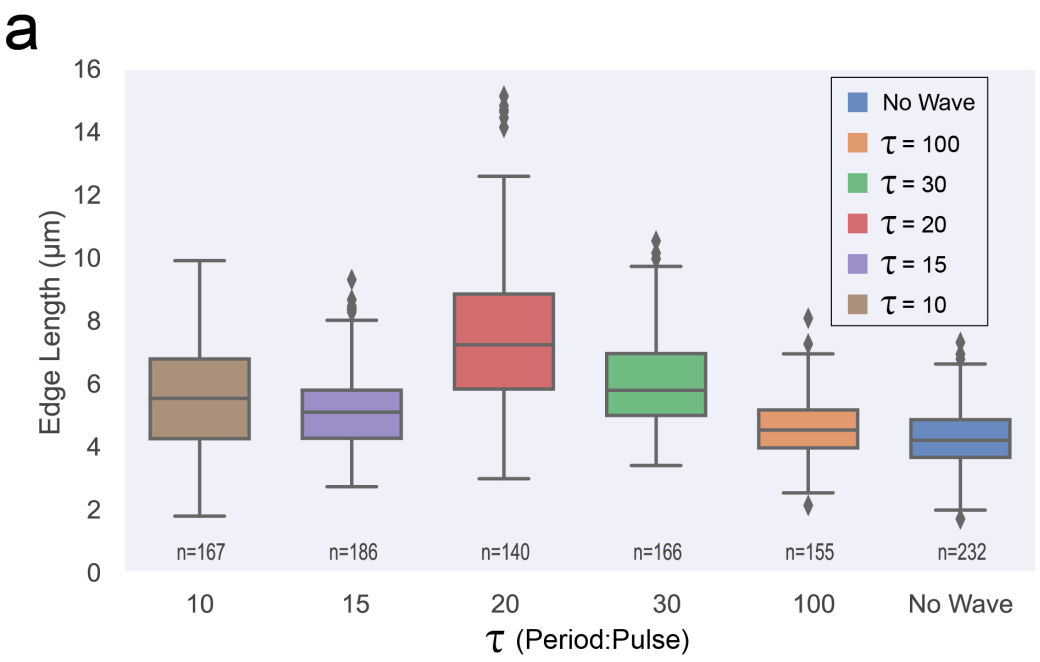

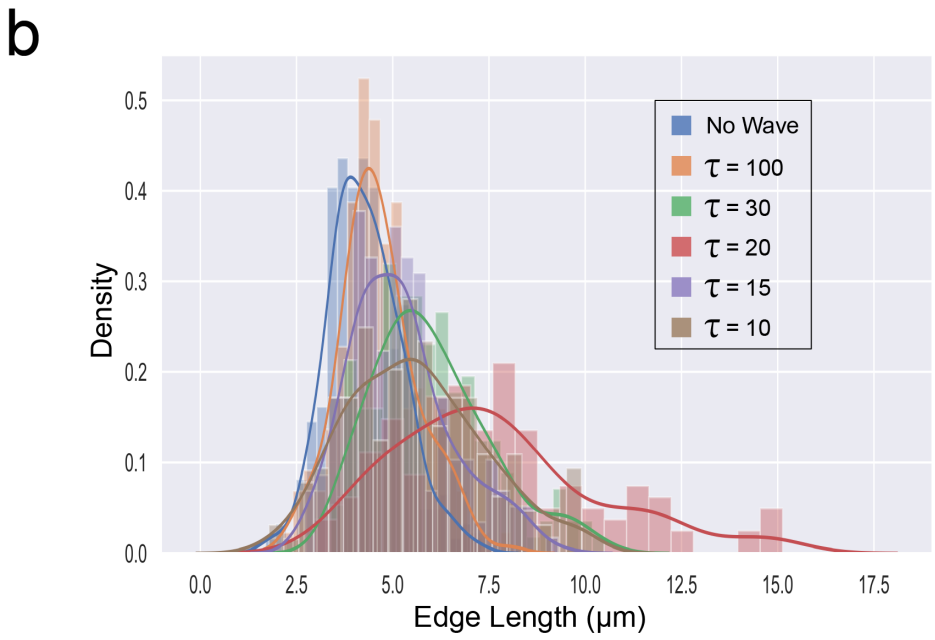

Supplementary Figure 6. **a.** Edge length box plot and distribution of crystals after formation with acoustic wave pulses with a '*fast*' temperature decrease rate of 0.03 °C/min. **b.** Edge length distribution of crystals after formation with acoustic wave pulses with a '*fast*' temperature rate of 0.03 °C/min.

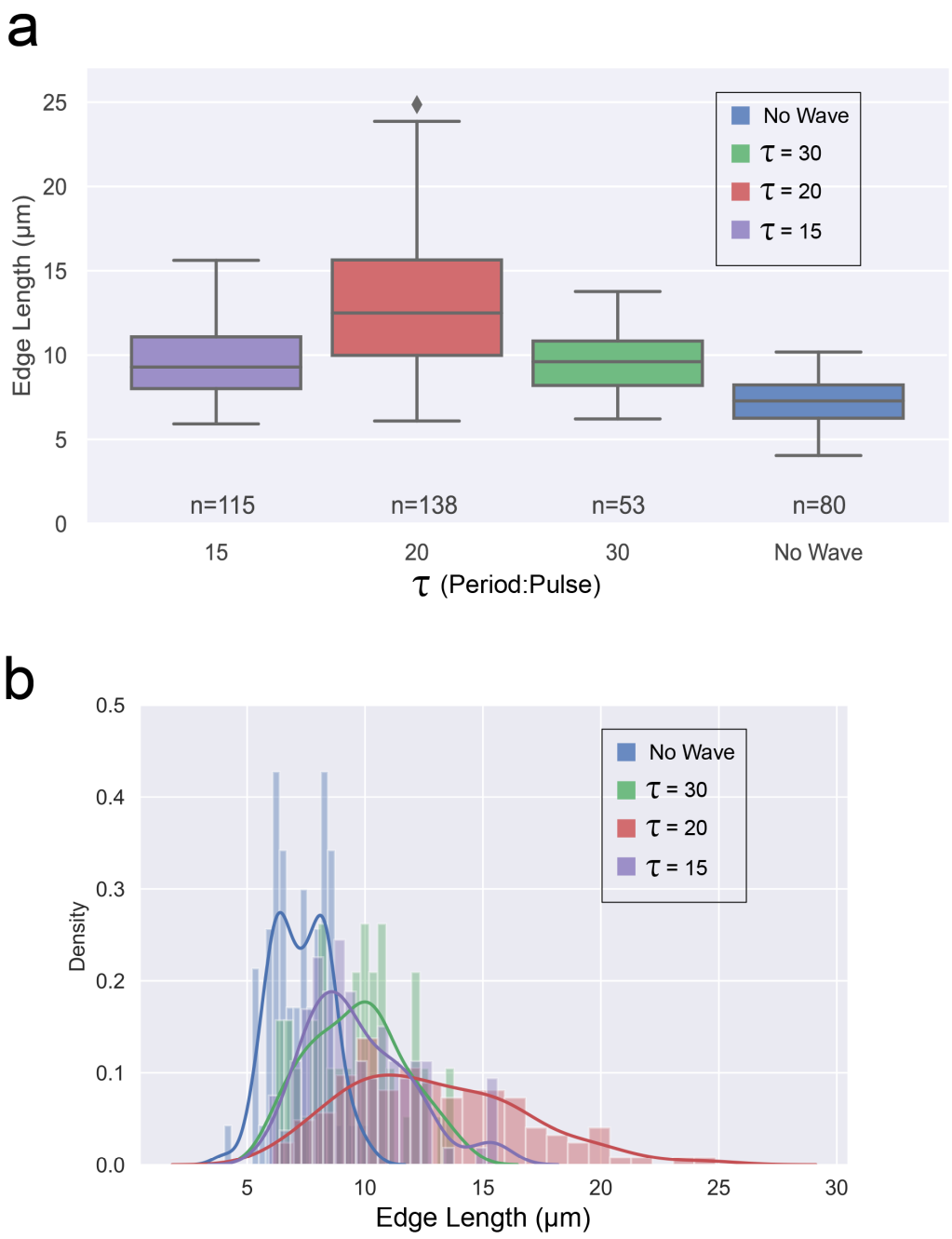

Supplementary Figure 7. **a.** Edge length box plot and distribution of crystals after formation with acoustic wave pulses with a '*slow*' temperature decrease rate of 0.01 °C/min. **b.** Edge length distribution of crystals after formation with acoustic wave pulses under a '*slow*' temperature rate of 0.01 °C/min.

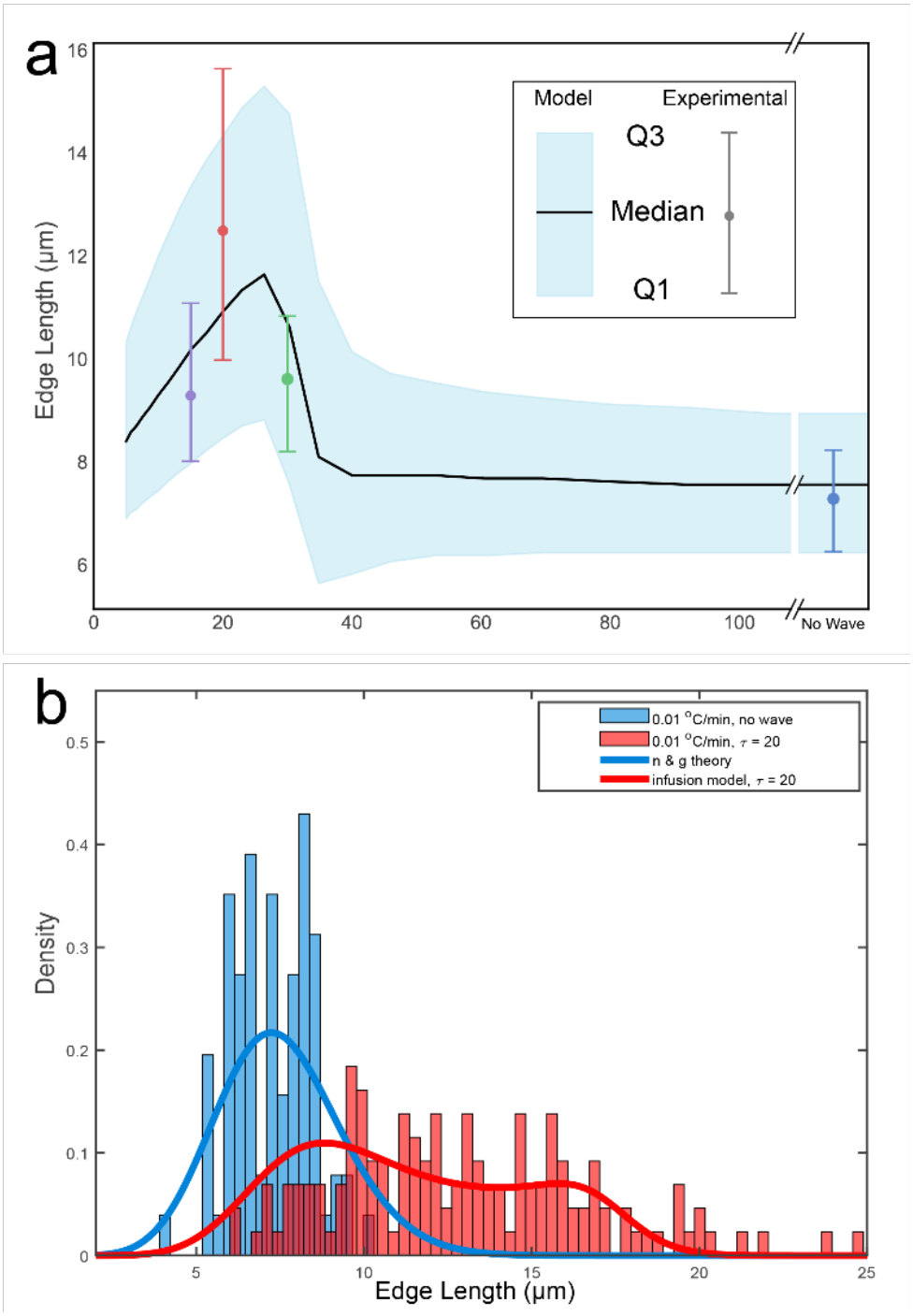

Supplementary Figure 8. **a.** Summary of crystal edge lengths vs. τ as calculated from the model and observed by the experimental data with a '*slow*' temperature ramp of 0.01 °C/min. **b.** Histogram of crystal size distribution with no acoustic waves (blue) and with $\tau = 20$ (red) for thermal ramp down of '*slow*' 0.01 °C/min. The nucleation and growth theoretical fit (blue line) and the infusion model (red line) take into consideration the effect of the acoustic field.

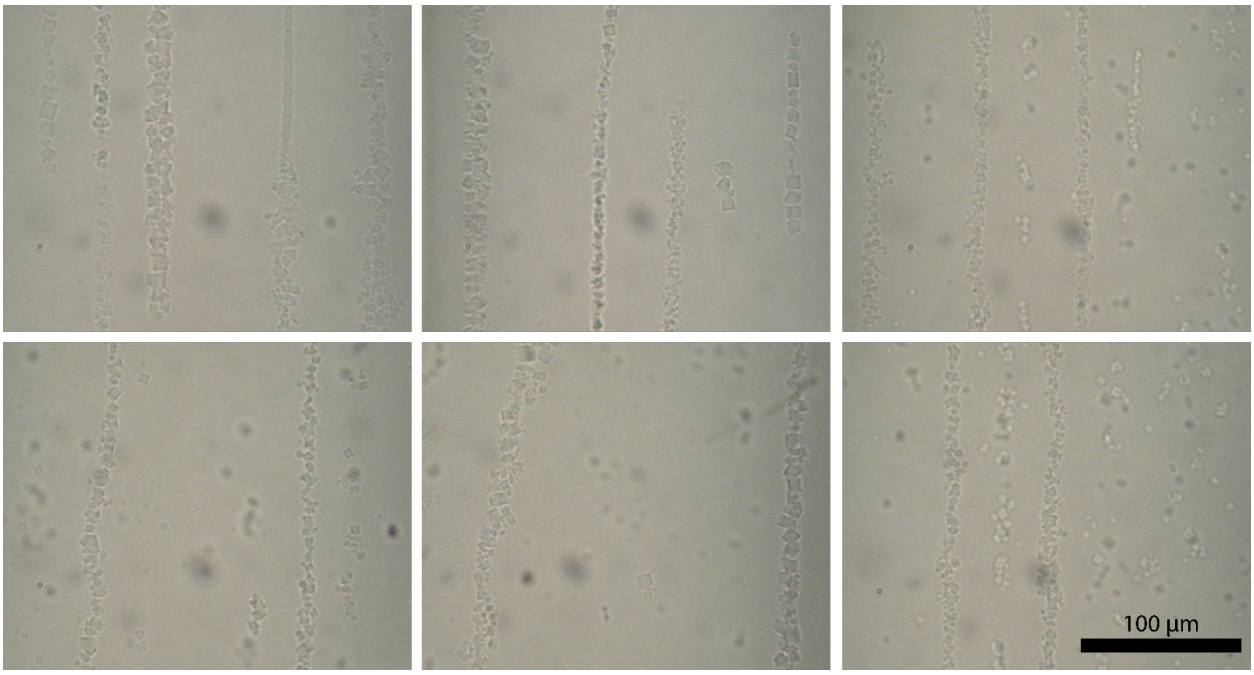

Supplementary Figure 9. Microscopy images of crystals after formation with acoustic wave pulses with a '*fast*' temperature decrease rate of 0.03 °C/min with an acoustic pulse every 500 ms (τ = 10).

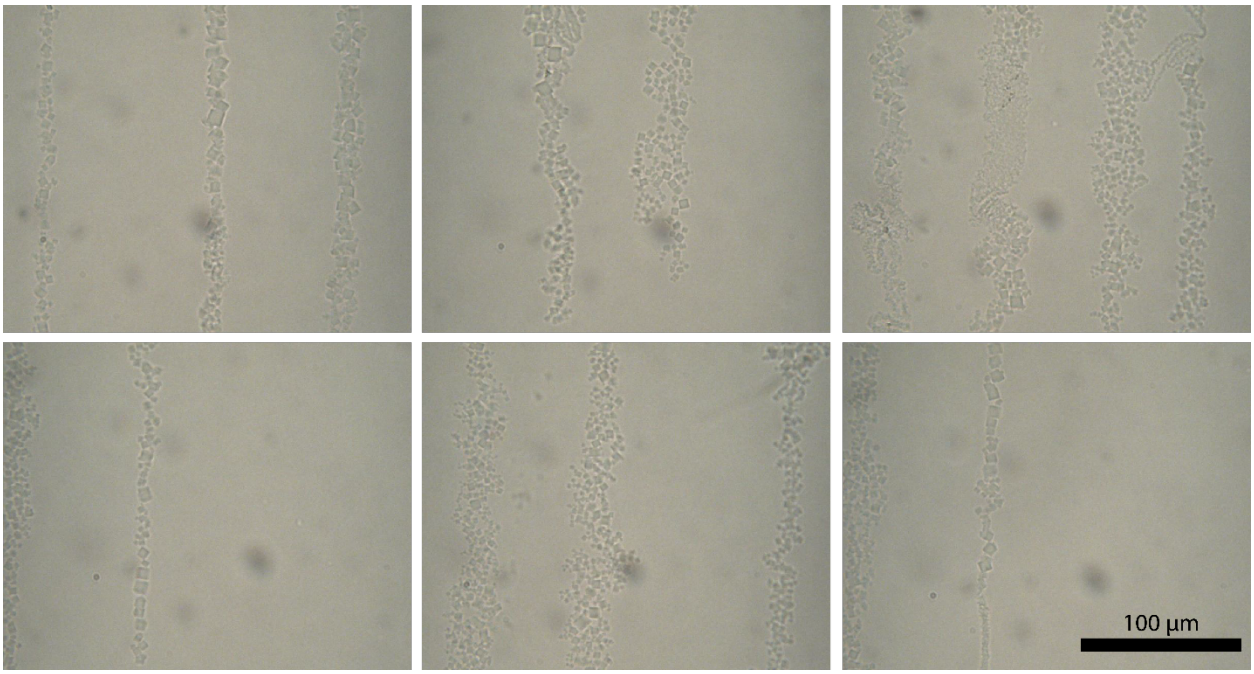

Supplementary Figure 10. Microscopy images of crystals after formation with acoustic pulses with a '*fast*' temperature decrease rate 0.03 °C/min with an acoustic pulse every 750 ms (τ = 15).

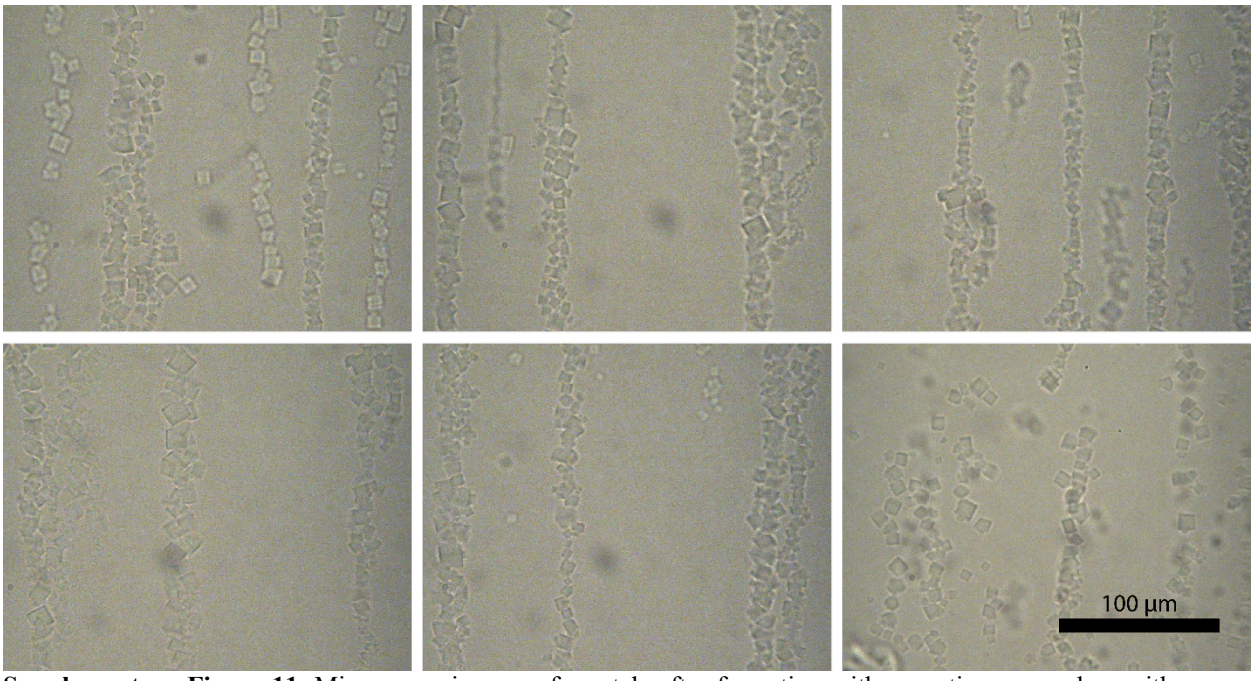

Supplementary Figure 11. Microscopy images of crystals after formation with acoustic wave pulses with a '*fast'* temperature ramp of 0.03 °C/min with an acoustic pulse every 1000 ms (τ = 20).

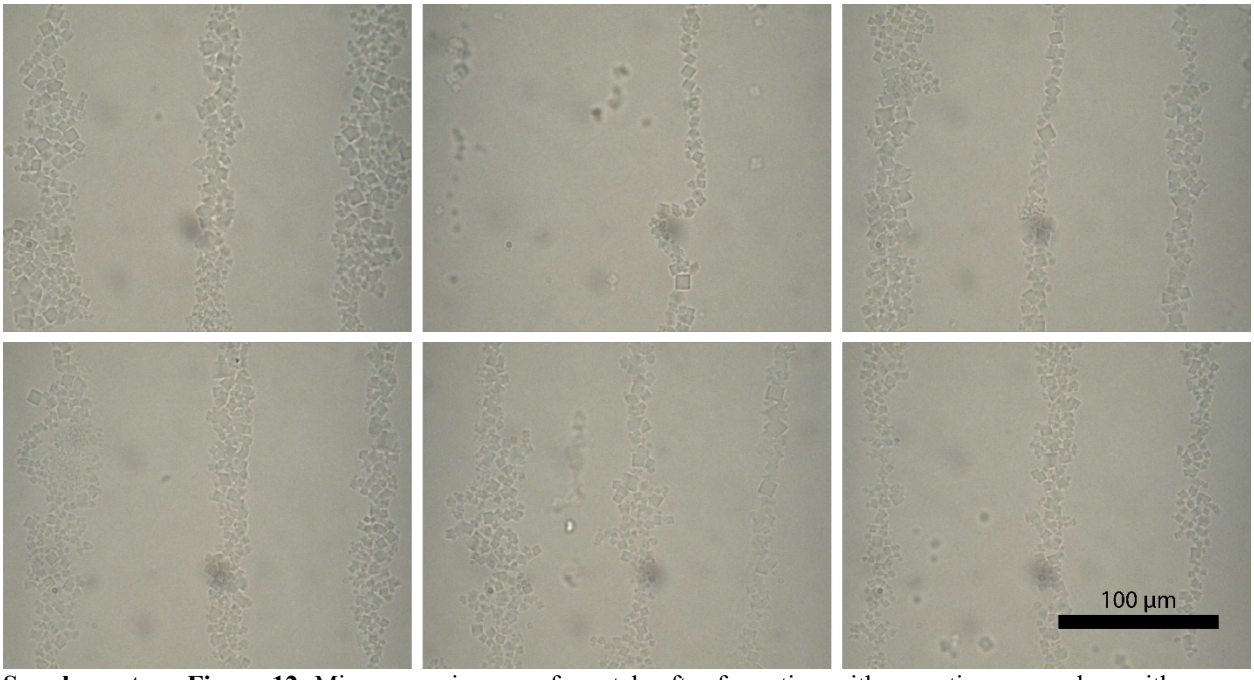

Supplementary Figure 12. Microscopy images of crystals after formation with acoustic wave pulses with a '*fast'* temperature decrease rate 0.03 °C/min with an acoustic pulse every 1500 ms (τ = 30).

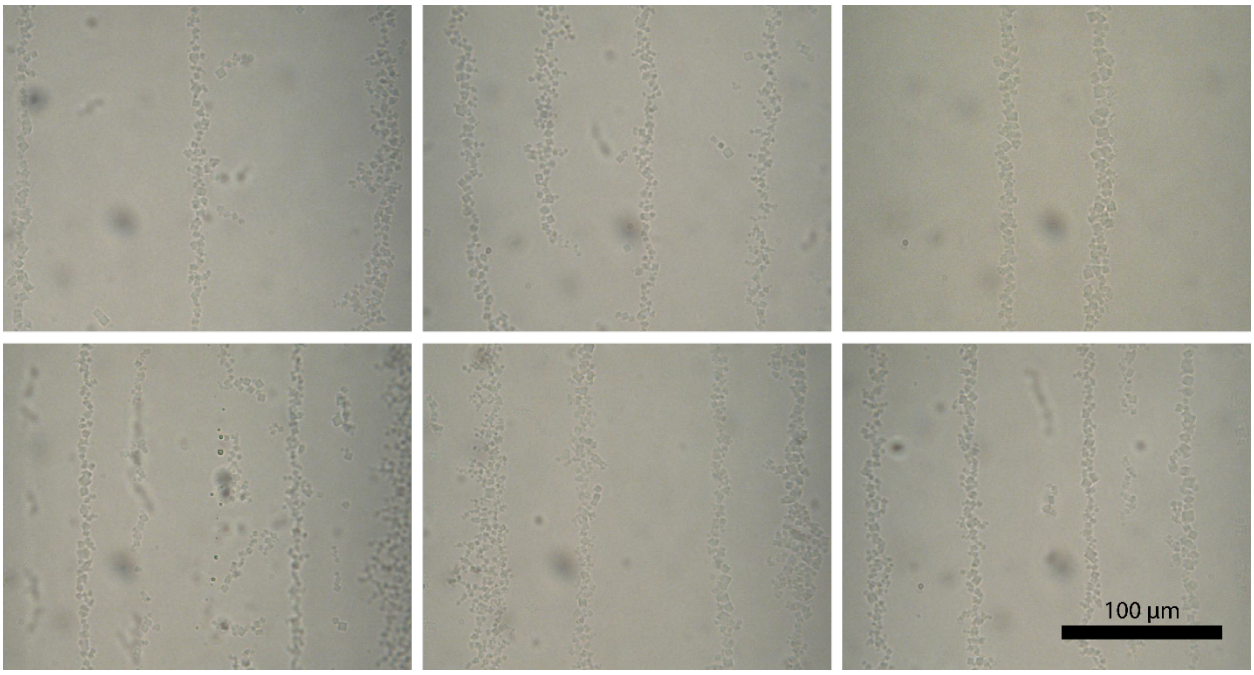

Supplementary Figure 13. Microscopy images of crystals after formation with acoustic wave pulses with a '*fast'* temperature decrease rate of 0.03 °C/min with an acoustic pulse every 5000 ms (τ = 100).

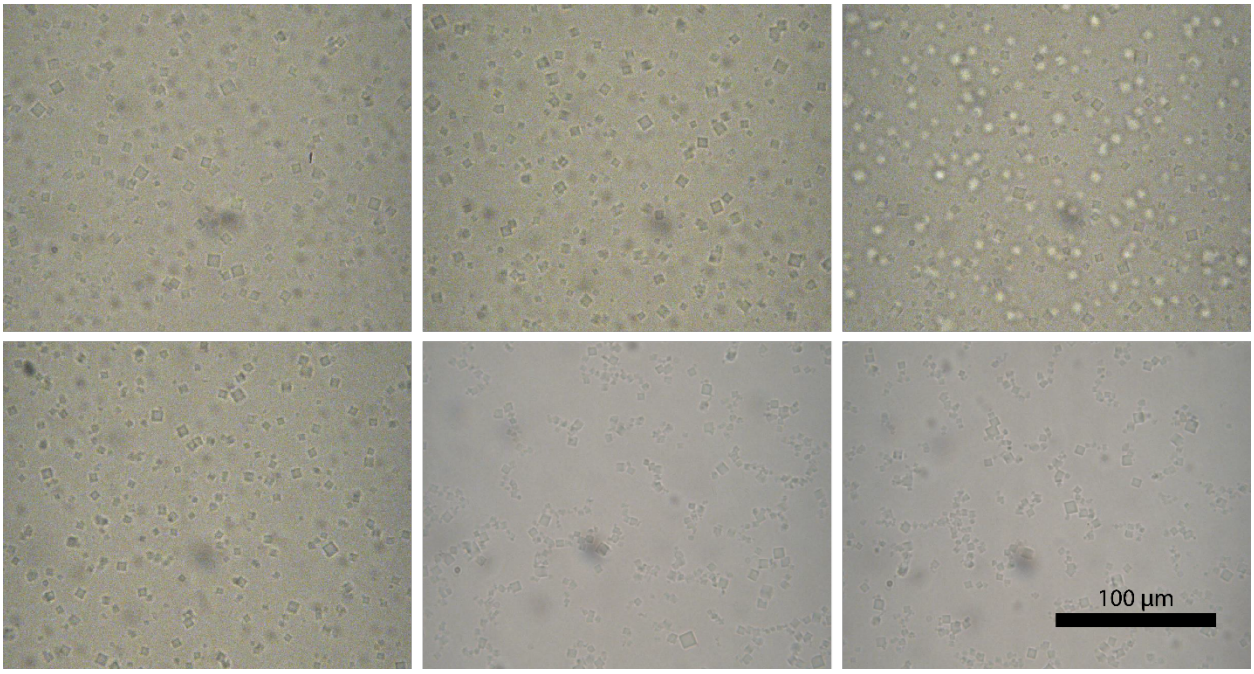

Supplementary Figure 14. Microscopy images of crystals after formation with no acoustic wave pulses with a '*fast'* temperature decrease rate of 0.03 °C/min (τ = ∞).

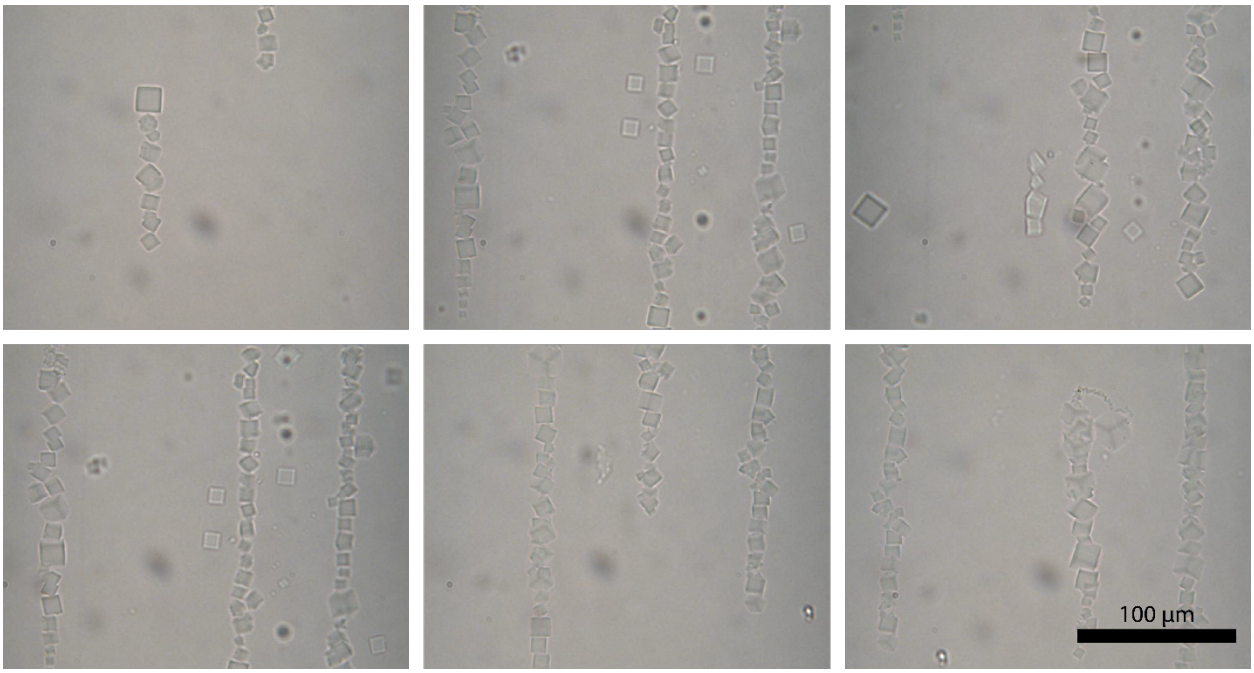

Supplementary Figure 15. Microscopy images of crystals after formation with acoustic wave pulses with a '*slow'* temperature decrease rate of 0.01 °C/min with an acoustic pulse every 750 ms (τ = 15).

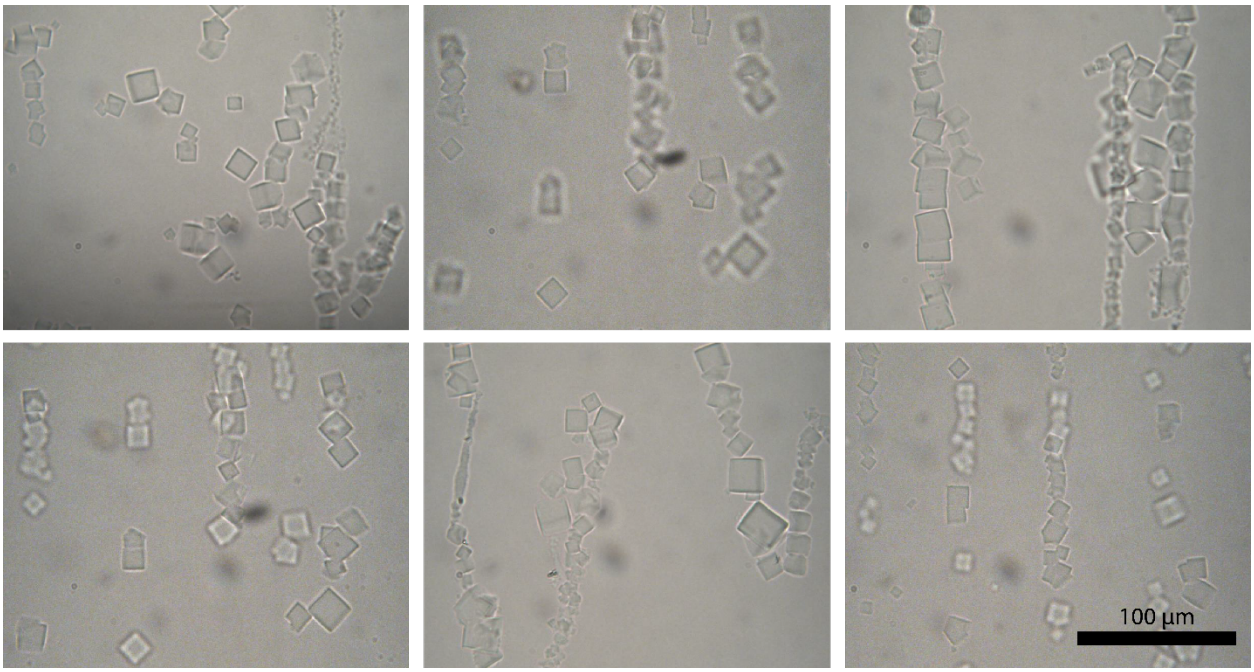

Supplementary Figure 16. Microscopy images of crystals after formation with acoustic wave pulses with a '*slow'* temperature decrease rate of 0.01 °C/min with an acoustic pulse every 1000 ms (τ = 20).

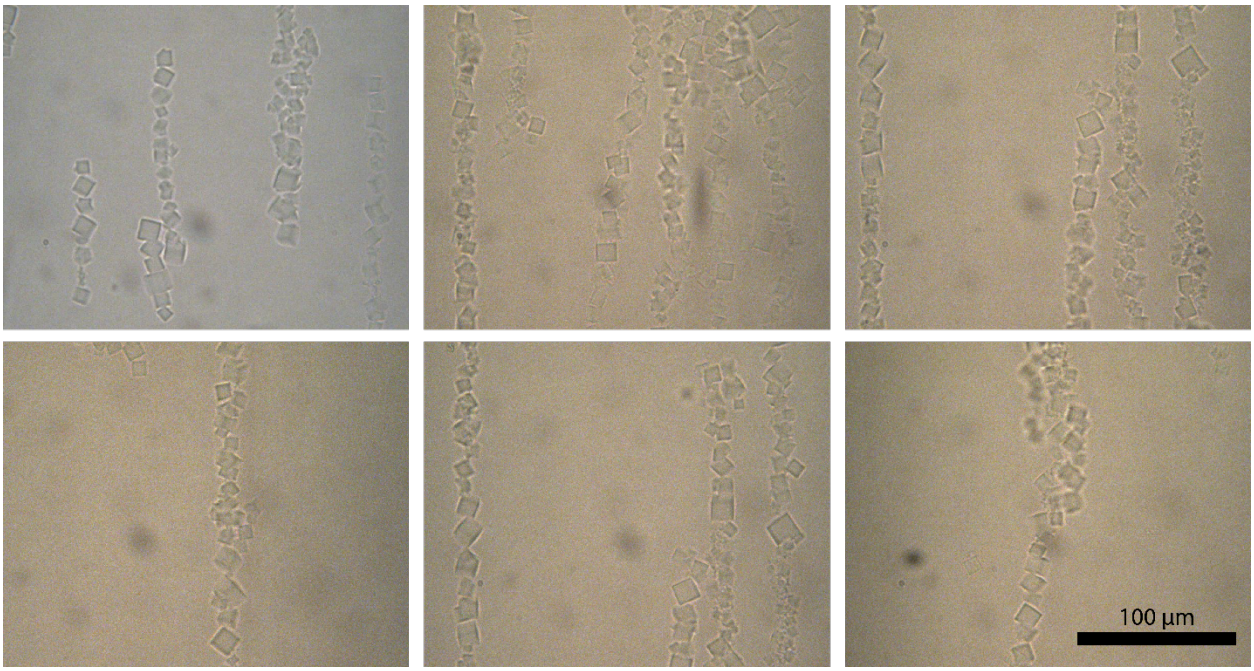

Supplementary Figure 17. Microscopy images of crystals after formation with acoustic wave pulses with a '*slow'* temperature decrease rate of 0.01 °C/min with an acoustic pulse every 1500 ms (τ = 30).

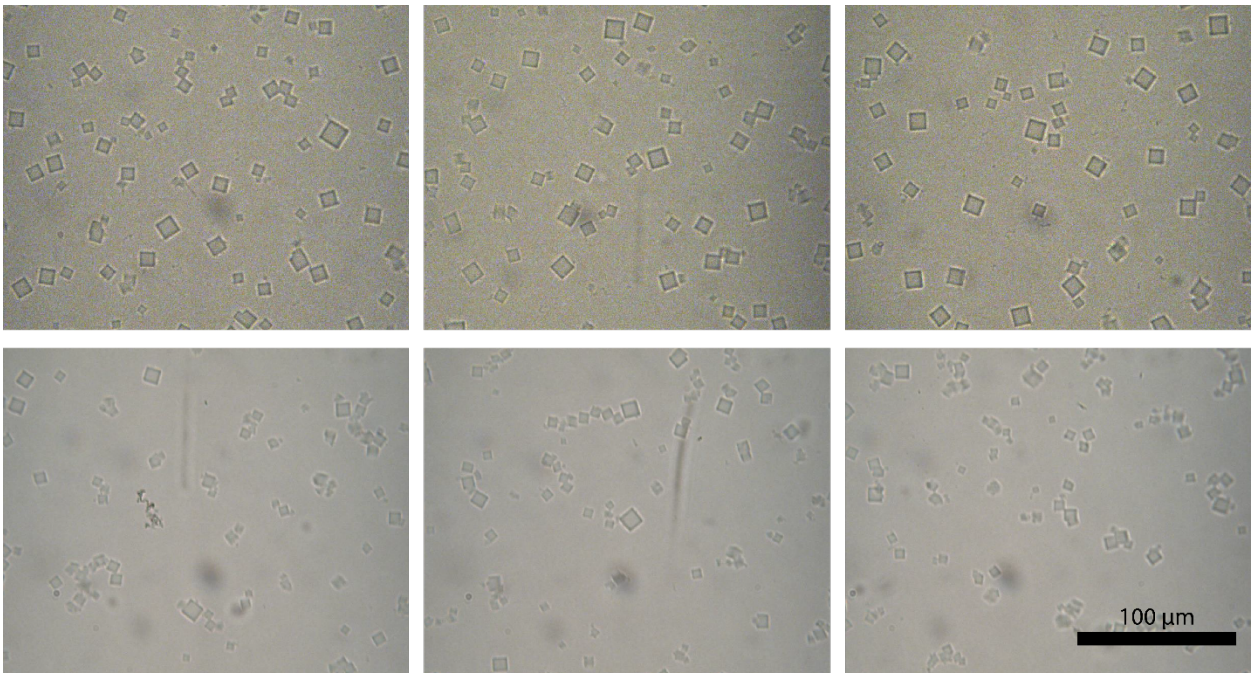

Supplementary Figure 18. Microscopy images of crystals after formation with no acoustic wave pulses with a '*slow'* temperature decrease rate of 0.01 °C/min ($\tau = \infty$).

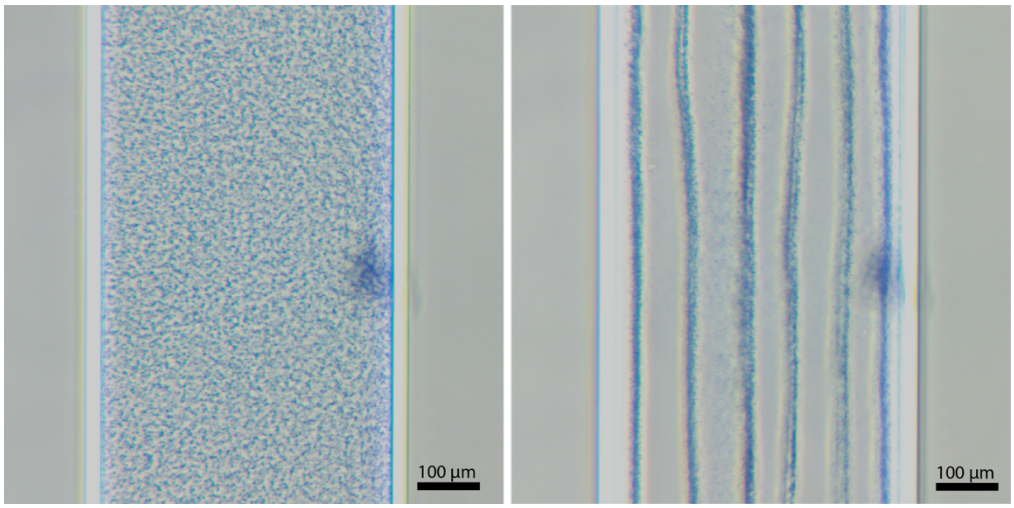

Supplementary Figure 19. Polysterene beads of 1 µm diameter, in a 1 mm wide capillary. The beads are dispersed in the capillary (left image) and then arranged by a pulse of 50ms acoustic waves every 1 seconcd (τ = 20). The corresponding video can be viewed in Supplementary Movies (Supplementary Movie 5).

Supplementary References

1. Schindelin, J. et al. Fiji: an open-source platform for biological-image analysis. Nat. Methods 9, 676–682 (2012).
2. Yager, K. G., Zhang, Y., Lu, F. & Gang, O. Periodic lattices of arbitrary nano-objects: modeling and applications for self-assembled systems. J. Appl. Crystallogr. 47, 118–129 (2014).
3. Yager, K.G., Zhang, Y., Lhermitte, J. ScatterSim (https://github.com/CFN-softbio/scattersim.).
4. Van Assche, D. Acoustophoretic manipulation of sub-micron particles. (2017).